Available online at www.CivileJournal.org

Civil Engineering Journal

(E-ISSN: 2476-3055; ISSN: 2676-6957)

Vol. 8, No. 01, January, 2022

High Strength Concrete Beams Reinforced with Hooked Steel Fibers under Pure Torsion

Haleem K. Hussain [1*], Mustafa Shareef Zewair [1], Mazin Abdulimam Ahmed [1]

[1] *Civil Engineering Department/ Engineering College, Basrah University, Basrah City, Iraq.*

Received 05 October 2021; Revised 11 December 2021; Accepted 21 December 2021; Published 01 January 2022

Abstract

A study of the behavior of fibers in high-strength reinforced concrete beams is presented in this paper. Twelve reinforced concrete beams were tested under a pure torsion load. Different compressive strengths (45.2, 64.7, and 84.8 MPa) and fiber volume fractions (0, 0.25, 0.5, and 0.75) with variable spacing between transverse reinforcements have been used. It was discovered that the maximum torque of a high-strength concrete beam is increased by about 20.3, 25.6, and 27.1% when the fractional volume of fiber is increased from 0 to 0.25, 0.5 and 0.75 respectively (when the compressive strength is 45.2 MPa and the transverse reinforcement spacing is 100 mm). The test results show that the ultimate torsional strength becomes higher when the concrete compressive strength increases, and this percentage increase becomes higher with increasing steel fiber volume fraction. When the spacing between transverse reinforcements decreases from 150 to 100 mm, the ultimate torque increases by 19.9%. When the spacing between transverse reinforcements decreases from 100 to 60 mm, the ultimate torque increases by 17.0%. In these beams, the fibers' compressive strength and volume fraction were kept constant at 45.2 MPa and 0.75, respectively.

Keywords: Torsion; Normal Strength Concrete; High Strength Concrete; Steel Fiber; Reinforcement.

1. Introduction

Steel fibers are recognized as a non-conventional mass reinforcement. They are currently being applied worldwide to strengthen structural concrete members because of their ability to enhance concrete mechanical properties and control crack propagation [1]. Steel fibers contribute to reducing the tensile stress transfer capability across crack surfaces. The principal benefit of discontinuous fibers in concrete is resisting and delaying crack propagation [2, 3]. Adding steel fibers to concrete can increase tensile strength, fracture energy absorption, and load-bearing capacity. The fibers can also enhance post-cracking behavior by improving stress transfer through fiber-bridging of cracked sections [4]. The post-cracking strength increases significantly with increased fiber-to-concrete ratios. The hooked ends of fibers can positively influence the pull-out behavior of concrete [5]. Ju et al. [6] introduced a constitutive model of steel fiber-reinforced concrete (SFRC) at the tension zone. This zone significantly affects torsional behavior, as shown by SFRC experimental results for shear panels under biaxial stress. The tensile behavior model adopted was a fixed-angle softened-truss model. After comparing the analytical results with other research, the study developed a theoretical evaluation for this type of SFRC torsional behavior model.

* Corresponding author: haleem.hussain@uobasrah.edu.iq; haleem.albremani@gmail.com

http://dx.doi.org/10.28991/CEJ-2022-08-01-07

Chalioris et al. [7] experimentally investigated concrete beams reinforced with hooked steel fibers under torsion. Their experimental program included 35 beams with different cross-sections (rectangular, L, and T shapes) tested under pure torsion for plain and reinforced (shear and bending) concrete beams. The beam test results demonstrated that beams with fibers enhance the torsional behavior compared to concrete without fiber. The researchers concluded that the addition of fibers prevented brittle failure. High strength concrete (HSC) offers many advantages over regular concrete, making it popular for various applications in the construction industry. The comparably higher compressive strength of HSC is an attractive advantage. However, high strength reduces the ductility of concrete by noticeably increasing its brittleness. Steel fibers added to reinforce HSC concrete increase its compressive strength without losing ductility [8].

Generally, the addition of steel fibers to concrete controls crack propagation and increases the ductility of the concrete. Hameed and Al-Sherrawi [9] investigated reinforced concrete beam behavior with steel-hooked end fibers for non-shear reinforcement beams. The results revealed that 1.0% volume fraction fiber could be used as an alternative material to restrict shear and increase the shear capacity of the beam. Fiber types other than steel, such as polypropylene and polyolefin based on polymer materials, have been recently used in a wide range of research areas. Denisiewicz et al. [10] experimentally tested fine-grained fiber concrete's mechanical and physical properties. Concrete prisms and cubes were selected to test with different steel and polypropylene fiber ratios. The results showed that using steel fiber improved shrinkage and compressive strength and did not deteriorate the workability compared with polypropylene fibers.

One of the main purposes of using steel fibers is to enhance the ductility of high-strength concrete (HSC). Research showed that steel fiber in reinforced concrete members greatly influenced the crack propagation mechanism. Experiments and FEM analyses of specimens had difficulty predicting the distribution of fibers in the concrete mix, which affected the accuracy of the results. Zhong et al. (2021) developed a theoretical model to evaluate the potential of using steel fibers as an alternative material to the normal steel reinforcement bars typically used. The study shows that increasing steel fiber volume in the concrete mixture improves the ductile performance, and these results confirmed recently published studies [11]. Facconi et al. (2021) studied large-scale reinforced concrete beams with steel fibers subjected to pure torsion. Normal reinforcement was used, and various stirrup quantities for transverse reinforcement were compared to beams without stirrups. Using steel fiber with a minimum reinforcement significantly increased the torsion capacity compared with the control specimen. Furthermore, SFRC provides a relatively high post-cracking stiffness compared to conventional reinforced concrete members [12].

Lau et al. (2020) [13] tested concrete beams subjected to pure torsional loads up to failure. The samples were alkali-activated concrete (AAC) beams. Three specimen types were the variables in the study: normal reinforced concrete, concrete with steel fiber only, and beams with normal reinforcement (steel bar) and steel fibers. The results showed that the AAC beam with only fibers had higher cracking torsion than the normal reinforced concrete beams. Also, the beam with normal reinforcement and steel fibers had a more ductile post-crack behavior. However, the hybrid reinforcements in alkali-activated concrete beams confirmed further consistent ductile post-crack behavior and improved ultimate torque capacity. Research related to fiber-reinforced HSC beams under pure torsion is minimal. The lack of experimental and analytical studies and the increasing interest in using steel fibers in HSC structures led to this study investigating the behavior of fiber-reinforced HSC beams under torsion. The tensile strength of non-reinforced concrete beam is low, it has a low strain capacity, and it is brittle material. Concrete properties, such as ductility, toughness, energy absorption, and strain at peak load, were increased using fiber reinforcement [2]. Fiber-reinforced concrete is made by combining cement, fibers with different properties, and aggregate in a composite material.

Studies with experimental evidence for torsion of fiber-reinforced high-strength concrete beams are very limited. This study experimentally examines the cracking strength, ultimate strength, and twist angle of fiber-reinforced high-strength beams subjected to pure torsion.

2. Martials and Method

The test program is intended to generate data and provide information and describe the effect of compressive strength, fiber volume fraction, and transverse reinforcement ratio on the behavior of fiber-reinforced high-strength beams subjected to pure torsion. Standard tests defined by the American Society for Testing and Materials (ASTM) [14-16] and Iraqi specifications [17, 18] are performed to conducting the material properties. These tests have been conducted at the laboratory of the Civil Engineering Department of Engineering College of Basrah University. The experimental work is depicted in Figure 1 as a flow chart.

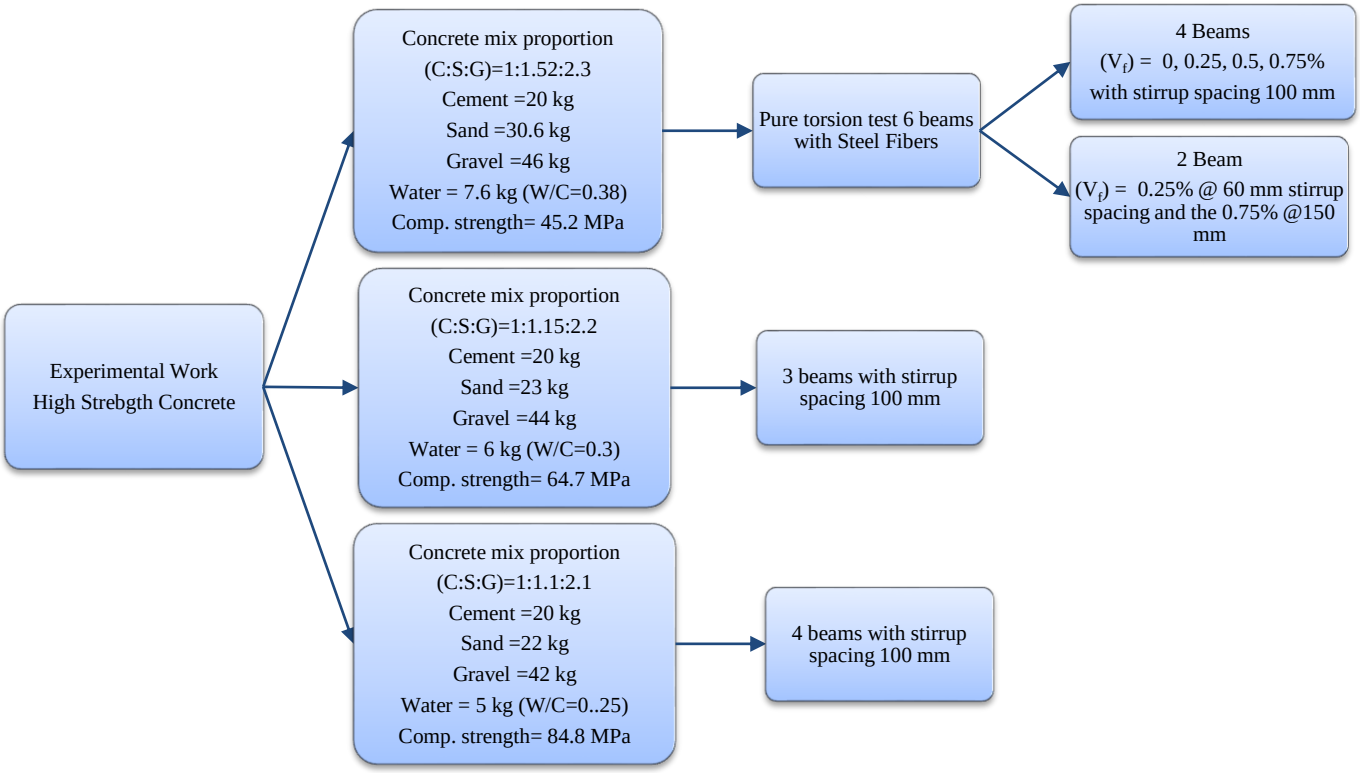

Figure 1. Flowchart of the methodology

2.1. Specimen Details

A total of twelve reinforced concrete beam specimens with a cross-sectional dimension of 200×200 mm with concrete cover equal to 20 mm were made-up at the laboratory. The overall length of the beam specimens was 1100 mm, and the test region length was 600 mm. All specimens had the same longitudinal reinforcement ratio but different shear reinforcement ratios. The beams were designed to vary the following parameters: compressive strength, fiber volume fractions ranging from 0 to 0.75, and steel shear ratio (spacing between transverse reinforcements). Table 1 and Figure 2 show additional beam specimen details.

Table 1. Beam Specimen Details

Specimen	Concrete	Longitudinal Reinforcement			Transverse Reinforcement		Fiber Reinforcement
	f_c (MPa)	No. of bar (Top)	No. of bar (Bottom)	f_{ly} (MPa)	D @ spacing	f_{wy} (MPa)	Volume Fraction V_f (%)
B1	45.2	2 D12	3 D16	520	D10@100	460	0
B2	45.2	2 D12	3 D16	520	D10@100	460	0.5
B3	45.2	2 D12	3 D16	520	D10@100	460	0.75
B4	45.2	2 D12	3 D16	520	D10@100	460	0.25
B5	45.2	2 D12	3 D16	520	D10@150	460	0.75
B6	45.2	2 D12	3 D16	520	D10@60	460	0.25
B7	64.7	2 D12	3 D16	520	D10@100	460	0
B8	64.7	2 D12	3 D16	520	D10@100	460	0.5
B9	64.7	2 D12	3 D16	520	D10@100	460	0.75
B10	84.8	2 D12	3 D16	520	D10@100	460	0
B11	84.8	2 D12	3 D16	520	D10@100	460	0.75
B12	84.8	2 D12	3 D16	520	D10@60	460	0.75

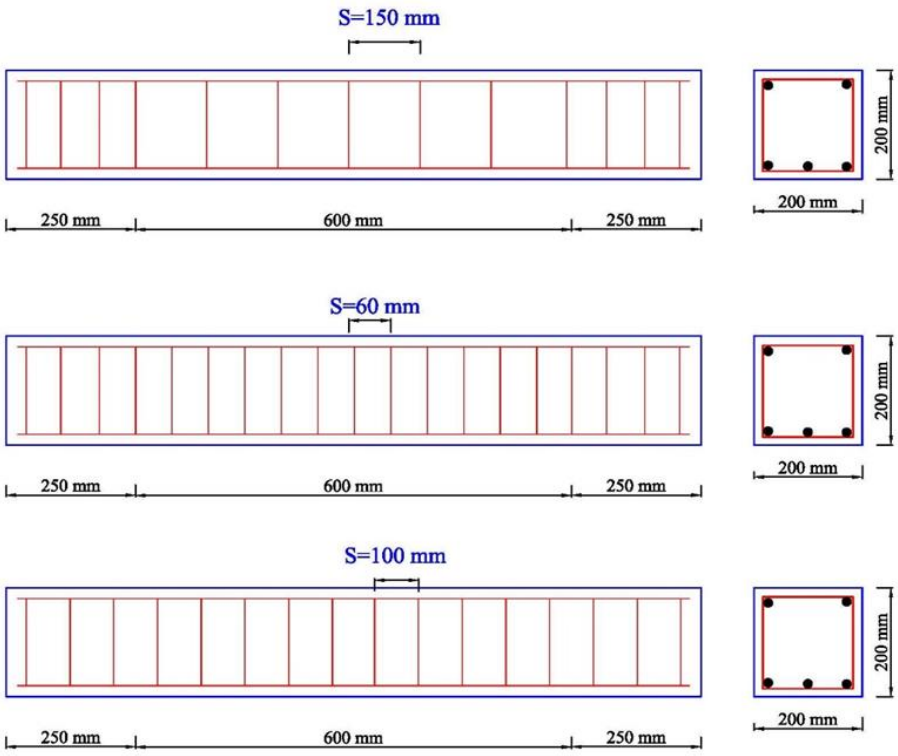

Figure 2. Beam Specimen Geometry Details

2.2. Material Properties

The concrete compressive strengths shown in Table 2 were found from the average of six 150× 150 mm standard cubic samples. The specimens were designed with 45, 65, and 85 MPa 28-day compressive strengths. Table 2 gives the concrete mix proportions for the different concrete strength values. Natural sand obtained from the Al-Zubair area in Basrah (Iraq) that complies with Iraqi Specification No. 45/1984 [18] was used as fine aggregate. The maximum crushed gravel size used was 12.5 mm. Figure 3 shows fine and coarse aggregate grading according to ASTM C33/86 [19]. Ordinary Portland cement was used for all three mixtures and conformed to Iraqi specification 5/1984 [17]. A high-performance concrete superplasticizer based on modified polycarboxylic ether manufactured, supplied by BASF® under the commercial name Degussa GLENIUM 54, was used as a water-reducing admixture. A nominal 1.2% of cement content superplasticizer dosage was used in all mixtures to achieve compatibility with the other materials. Hooked edge steel fibers were added to all mixtures with volume fractions ranging from 0 to 0.75, as shown in Figure 4.

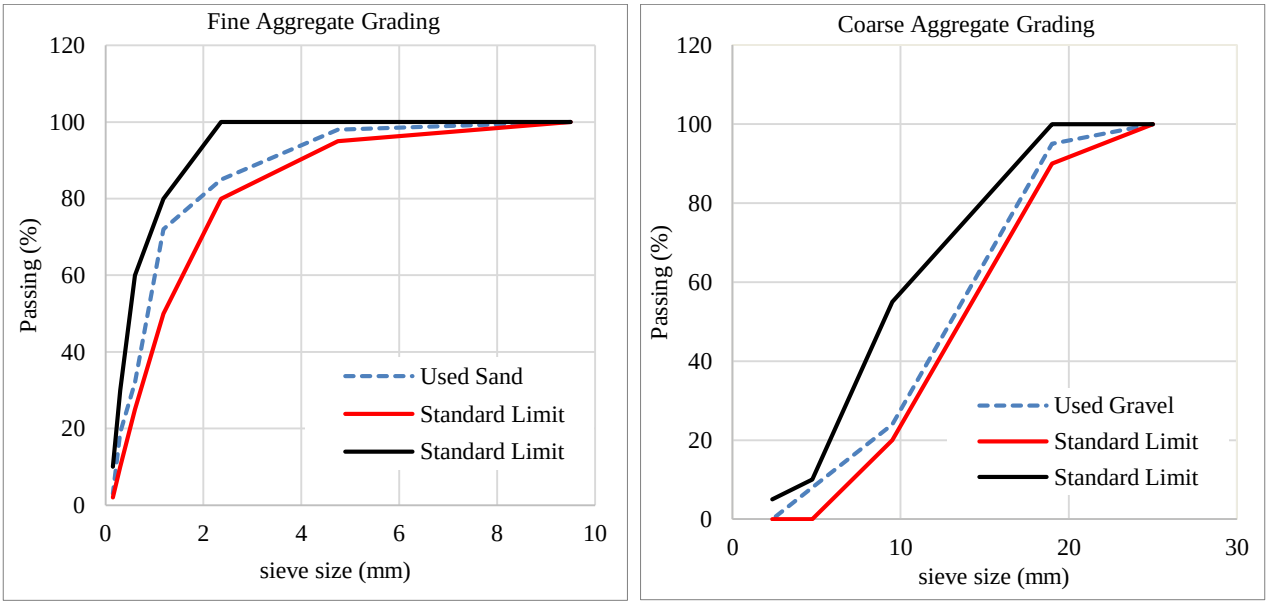

Figure 3. Coarse and Fine Aggregate Grading

Table 2. Concrete Mixture Proportions

Components	Concrete Mix Proportions		
	45.2 MPa	**64.7 MPa**	**84.8 MPa**
	1:1.53:2.3	1:1.15:2.2	1:1.1:2.1
Cement, kg	20	20	20
Water, kg	7.6	6	5
W/C	0.38	0.3	0.25
Fine Aggregate, kg	30.6	23	22
Coarse Aggregate, kg	46	44	42
High-ranger Water Reducing Admixture	0.24	0.24	0.24

Figure 4. Hooked Steel Fibers

2.3. Test Setup and Devices

Figure 5 shows the details of the test setup. The test setup was designed and constructed to apply a torsional moment on the beam specimens. The steel frames were fixed firmly at the ends of the beam specimens to produce the torsional arm, and the net length of the torsion lever arm was 0.65 m. The beams were designed to be simply supported at two bearings, where the roller supports were installed under the bearing to release the restraint of the beam specimens. This design allowed the beam to rotate easily under the applied torque throughout the test. Using a hydraulic universal testing machine, a normal load applied to the torsional arm through a spreader beam produced the torque.

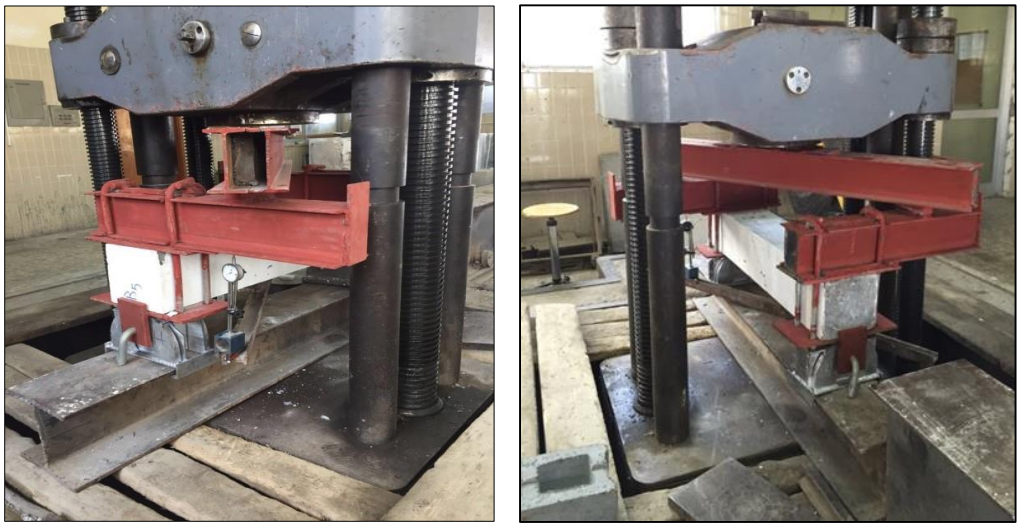

Figure 5. Schematic of Test Setup

2.4. Test Procedure

All of the specimens were loaded gradually which lead to increasing the torque until failed. A trial test was conducted before testing the specimens. The beam was loaded to failure in the trial test, verifying the loading test instruments and collecting data that was checked to guarantee acceptable accuracy. After performing the trial test, the actual tests were carried out. Beams were gradually loaded, and at each load increment, readings were manually recorded.

2.5. Twist Angle Measurements

To inspect the angle of twist, a couple of dial gauges located at 650 mm from the center of longitudinal axis of reinforced concrete beam, the dial gauges fixed at the ends of beam at the bottom fiber of the lever arm as shown in Figure 5. The twist angle in radian was find, by taking the average of values recorded from a dial gage on the left and on right.

3. Results and Discussion

Table 3 shows the principal test results, while the torque versus twist angle curves for the high-strength concrete beams are provided in Figure 6.

Table 3. Principal Test Results

Specimen	Compressive Strength, f_c' (MPa)	Steel Fibers (Vf)	Spacing between transverse reinforcement (mm)	Torsional Moment (Tu), (kN.m)	Increasing load According to B1 Beam (%)	Angle of Twist (ϕ) (rad.)
B1	45.2	0	100	24.68	----	0.01923
B2	45.2	0.5	100	30.99	25.6	0.02530
B3	45.2	0.75	100	31.37	27.1	0.02600
B4	45.2	0.25	100	29.69	20.3	0.02400
B5	45.2	0.75	150	26.17	6.0	0.02250
B6	45.2	0.25	60	34.74	40.8	0.02640
B7	64.7	0	100	35.66	44.5	0.02600
B8	64.7	0.5	100	38.83	57.3	0.03200
B9	64.7	0.75	100	39.64	60.6	0.03328
B10	84.8	0	100	42.01	70.2	0.03250
B11	84.8	0.75	100	46.29	87.6	0.03900
B12	84.8	0.75	60	52.03	110.8	0.04200

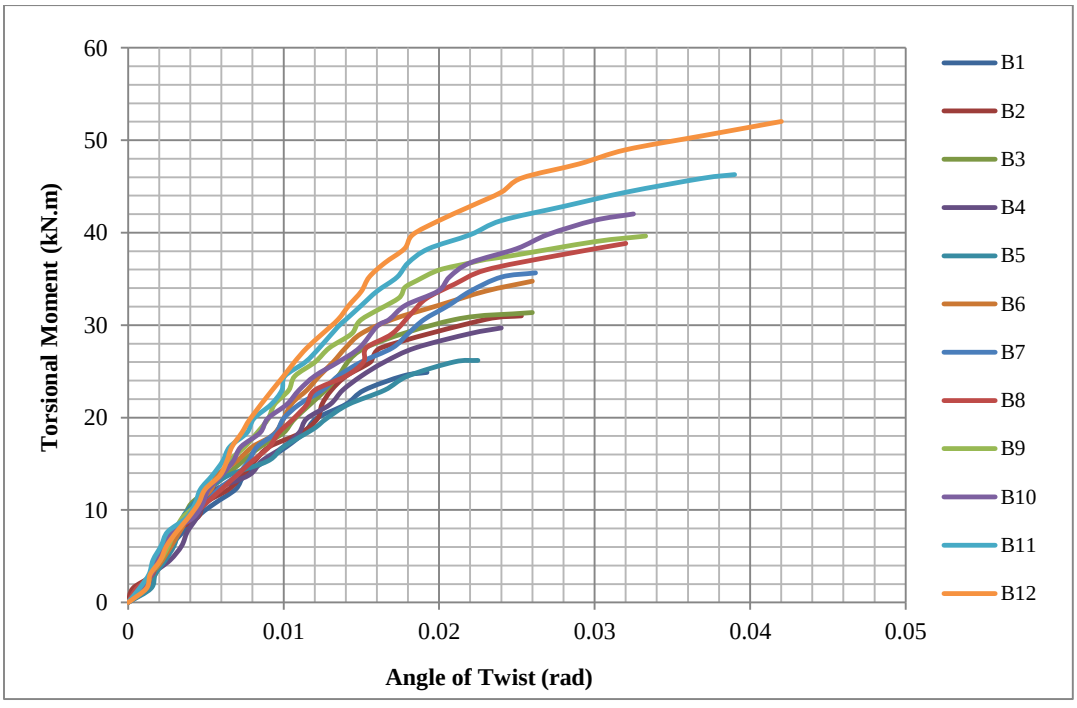

Figure 6. Torque-twist Relationships for High-Strength Concrete Beams

3.1. Effect of Concrete Strength on Ultimate Strength

Figure 7 and Table 4 show the effect of the torsional moment versus twisting angle for HSC beams B1, B7, and B10 with compressive strengths of 45.2, 64.7, and 84.8 MPa, respectively. The transverse reinforcement was constant (S = 100 mm), and the fiber volume fraction was Vf = 0, Results for Vf = 0.75 (beams B3, B9, and B11) are given in Figure 8 and Table 5.

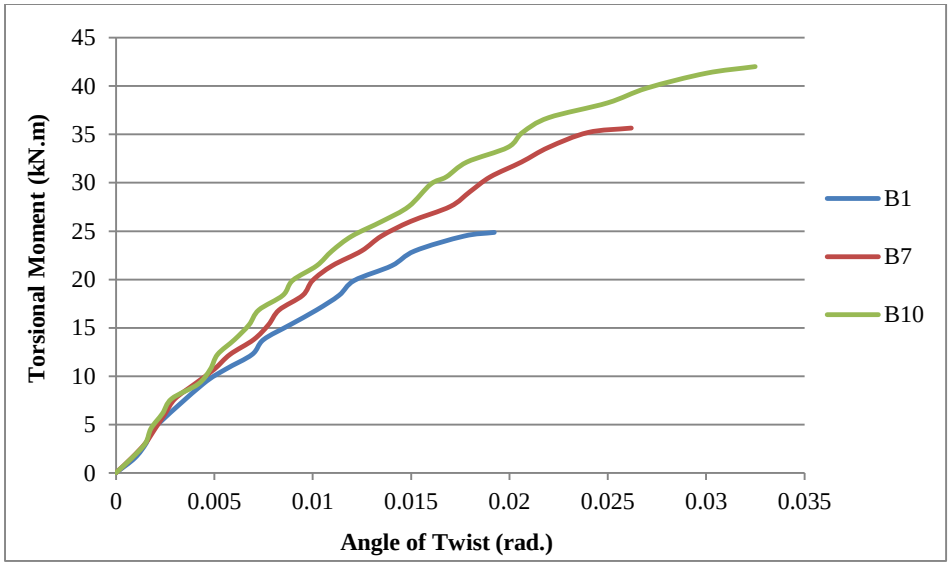

Figure 7. Torque-Twist Behavior of HSC Beams B1, B7, and B10

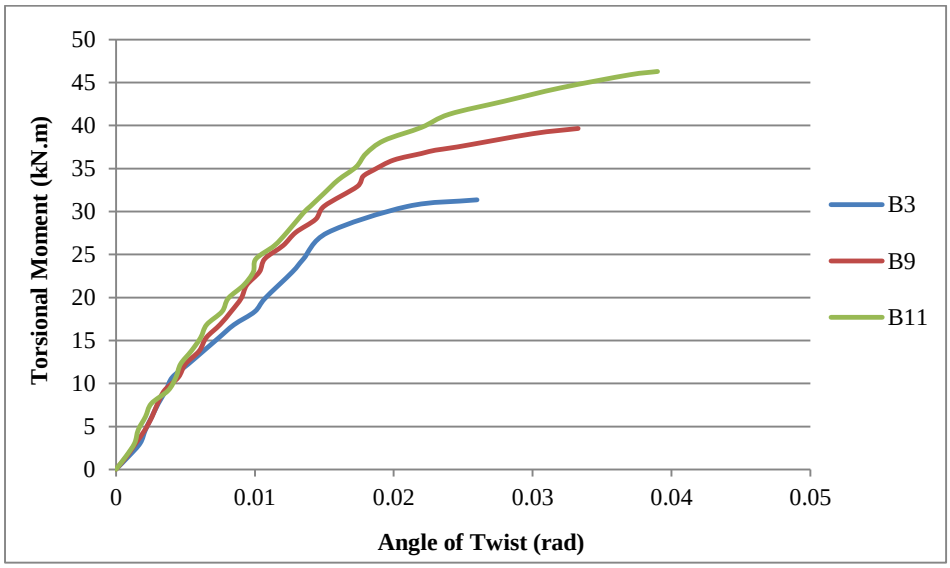

Figure 8. Torque-Twist Behavior of HSC Beams B3, B9, and B11

Table 4. Effect of Variation in Compressive Strength on Ultimate Torque and Twist Angle of HSC Beams B1, B7, and B10

Specimen	Compressive strength (MPa)	Volume Fraction of Fibers (%)	Spacing (mm)	Ultimate Torque (kN.m)	Percent of Increase (%)	Angle of Twist (ϕ) (rad.)	Percent of Increase (%)
B1	45.2	0	100	24.68	---	0.01923	---
B7	64.7	0	100	35.66	44.5	0.02600	35.2
B10	84.8	0	100	42.00	70.2	0.03250	69.0

Table 5. Effect of Variation in Compressive Strength on Ultimate Torque and Twist Angle of HSC Beams B3, B9, and B11

Specimen	Compressive strength (MPa)	Volume Fraction of Fibers (%)	Spacing (mm)	Ultimate Torque (kN.m)	Percent of Increase (%)	Angle of Twist (ϕ) (rad.)	Percent of Increase (%)
B3	45.2	0.75	100	31.37	---	0.02600	---
B9	64.7	0.75	100	39.64	26.4	0.03328	28.0
B11	84.8	0.75	100	46.29	47.6	0.03900	50.0

From these data, as the compressive strength increases from 45.2 to 64.7 and 84.8 MPa, respectively, the ultimate torque increases by 44.5% and 70.2%. The twist angle was increased by 35.2% and 69.0%, respectively, and the angle of twisting increased by 26.4% and 47.6%, respectively. These results imply that the concrete strength significantly affects the ultimate torque and twist angle.

3.2. Effect of Fiber Volume Fraction

Figure 9 shows the behavior of HSC beams with fiber volume fractions of 0, 0.5, 0.75, and 0.25, respectively. The compressive strength and spacing between transverse reinforcements for the tested beams in Figure 9 were f'c = 45.2 MPa and S = 100 mm, respectively. Figure 10 shows the behavior of HSC beams with steel fiber ratios of 0, 0.5, and 0.75 for specimens with compressive strength f'c = 64.7 MPa and transverse reinforcement spacing S = 100 mm.

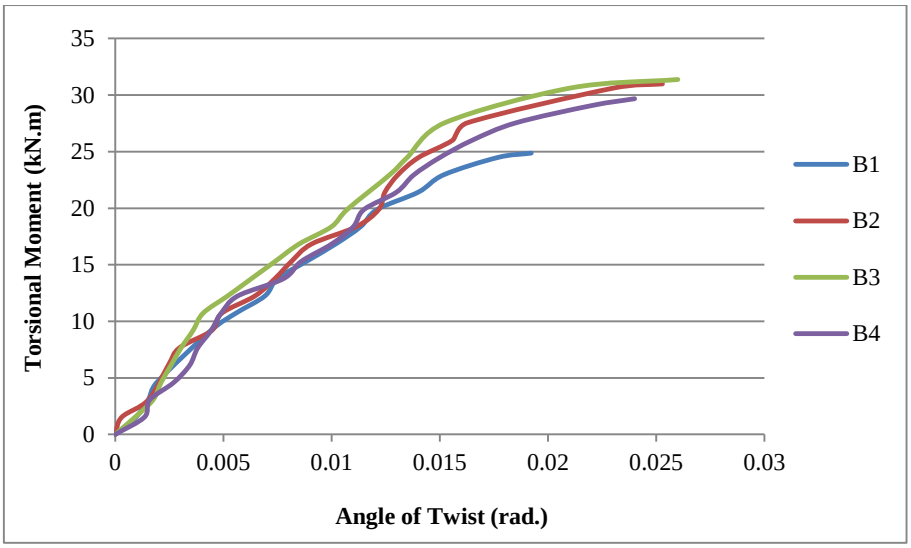

Figure 9. Torque-Twist Angle of HSC Beams

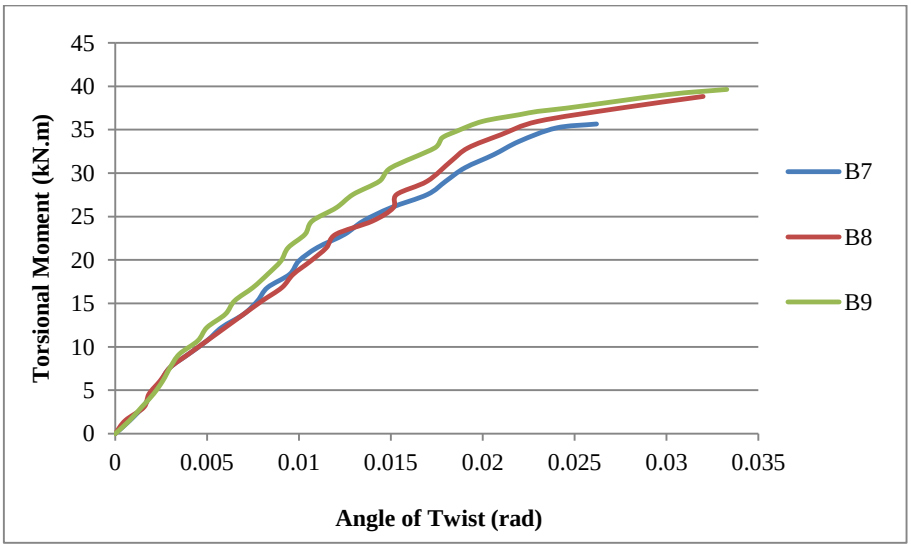

Figure 10. Torque-Twist Angle Behavior of HSC Beams

Table 6 shows the maximum applied torque increase as the steel fiber ratio increases. The ultimate torque was found to increase by 20.3, 25.6, and 27.1% as the fiber ratio increased from 0 to 0.25, 0.5, and 0.75, respectively. In Table 7, the ultimate torque increases by 8.9 and 11.2% when fiber volume fraction increases from 0 to 0.5 and 0.75, respectively.

Table 6. Effect of variation in compressive strength on ultimate torques and angle of twist of HSC Beams B1, B2, B3, B4.

Specimen	Compressive strength (MPa)	Volume Fraction of Fibers (%)	Spacing (mm)	Ultimate Torque (kN.m)	Percent of Increase (%)	Angle of Twist (ϕ) (rad.)	Percent of Increase (%)
B1	45.2	0	100	24.68	---	0.01923	---
B2	45.2	0.5	100	30.99	25.6	0.02530	31.6
B3	45.2	0.75	100	31.37	27.1	0.02600	35.2
B4	45.2	0.25	100	29.69	20.3	0.02400	24.8

Table 7. Effect of variation in compressive strength on ultimate torques and angle of twist of HSC Beams B7, B8, and B9.

Specimen	Compressive strength (MPa)	Volume Fraction of Fibers (%)	Spacing (mm)	Ultimate Torque (kN.m)	Percent of Increase (%)	Angle of Twist(ϕ) (rad.)	Percent of Increase (%)
B7	64.7	0	100	35.66	---	0.02600	---
B8	64.7	0.5	100	38.83	8.9	0.03200	23.1
B9	64.7	0.75	100	39.64	11.2	0.03328	28.0

In the non-fibrous beams, diagonal cracking is followed by a limited post-cracking load capacity due to the presence of stirrups. Failure is then attained by a gradual widening of the diagonal crack. However, the diagonal cracking torque and the ultimate torque were substantially increased when steel fibers were added. In that case, the failure occurred by diagonal crack widening and stirrup yielding but had a more gradual nature and was accompanied by numerous fine cracks at the diagonal failure region surface. This behavior is primarily due to the presence of fibers across the diagonal failure surface, which obstruct crack propagation and tend to bind the crack on opposite sides of the failure surface. Therefore, numerous diagonal cracks were detected at the external faces of all concrete beams with fibers, especially when the percentage of fibers was high. These cracks indicated stress redistribution after cracking and the continued resistance to tensile stresses until a complete pull-out of all fibers occurred at the critical crack.

3.3. Effect of Transverse Reinforcement Ratio

Figure 11 shows the torque versus twist angle curves of HSC beams B3 and B5 with transverse reinforcement spacings of 100 mm and 150 mm, respectively. The compressive strength and fiber volume fraction were constant for these beams at f'c = 45.2 MPa and V_f = 0.75, respectively. Figure 12 shows the torque versus twist curves of HSC beams B4 and B6 with transverse reinforcement spacings of 100 mm and 60 mm, respectively. For beams B4 and B6, the compressive strength and fiber volume fraction of fibers were kept constants at f'c = 45.2 MPa and V_f = 0.25, respectively. The torque versus twist angle curves of HSC beams B11 and B12 with transverse reinforcement spacings of 100 mm and 60 mm, respectively, are shown in Figure 13. The compressive strength and fiber volume fraction for beams B11 and B12 were constant at f'c = 84.8 MPa and V_f = 0.75, respectively. Tables 8 to 10 show the effect of different transverse reinforcement spacings on the ultimate torques and angles of twist of these beams.

Table 8 shows that when the spacing between transverse reinforcements decreases from 150 mm to 100 mm, the ultimate torque increases by 19.9%. When this spacing is reduced from 100 mm to 60 mm, the ultimate torque rises by 17.0%, as shown in Table 9. Table 10 reveals that when the transverse reinforcement spacing decreases from 100 mm to 60 mm, the ultimate torque increases by 12.4%.

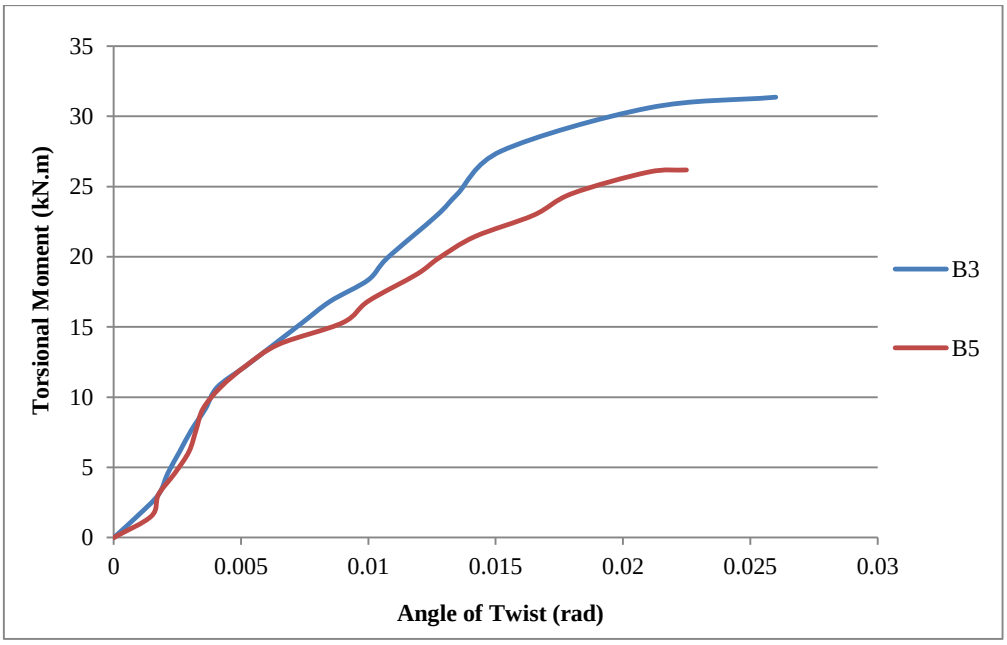

Figure 11. Torque-Twist Angle of High Strength Concrete Beams B3 and B5

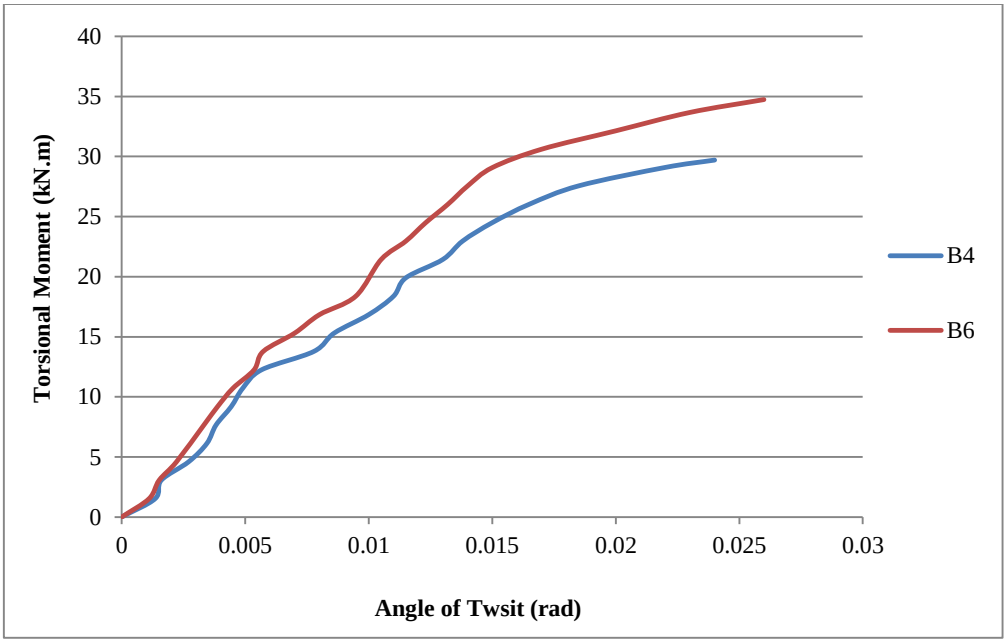

Figure 12. Torque-Twist Angle of High Strength Concrete Beams B4 and B6

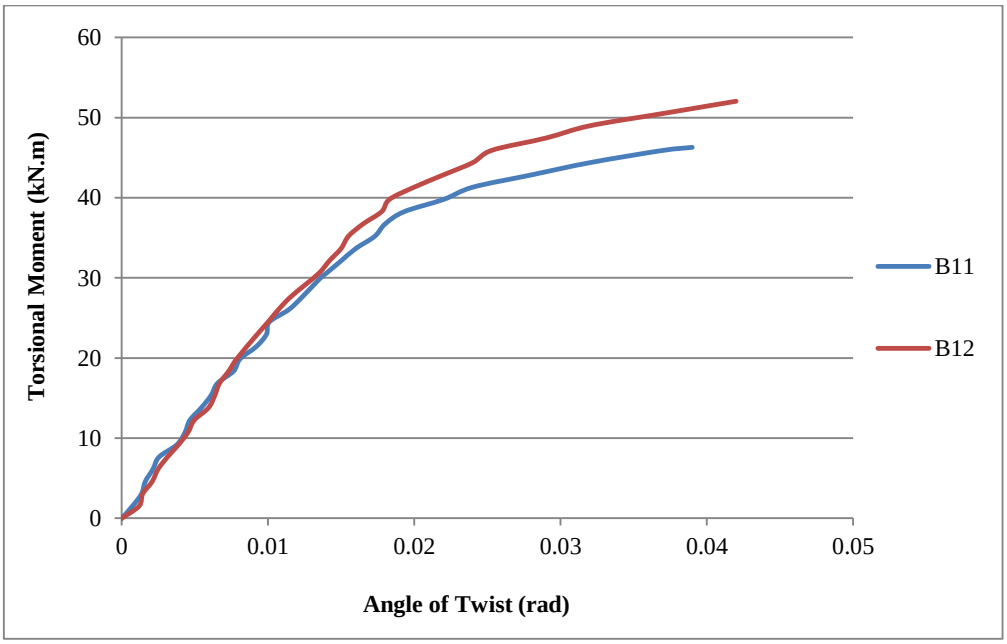

Figure 13. Torque-Twist Angle High Strength Concrete Beams B11 and B12

Table 8. Effect of change in spacing between transverse reinforcement on the ultimate torques and angle of twist of HSC Beams B3 and B5

Specimen	Compressive strength (MPa)	Volume Fraction of Fibers (%)	Spacing (mm)	Ultimate Torque (kN.m)	Percent of Increase (%)	Angle of Twist (ϕ) (rad.)	Percent of Increase (%)
B3	45.2	0.75	100	31.37	19.9	0.02600	15.6
B5	45.2	0.75	150	26.17	---	0.02250	---

Table 9.Effect of change in spacing between transverse reinforcement on the ultimate torques and angle of twist of HSC Beams B4 and B6

Specimen	Compressive strength (MPa)	Volume Fraction of Fibers (%)	Spacing (mm)	Ultimate Torque (kN.m)	Percent of Increase (%)	Angle of Twist (ϕ) (rad.)	Percent of Increase (%)
B4	45.2	0.25	100	29.69	---	0.02400	---
B6	45.2	0.25	60	34.74	17.0	0.02640	10.0

Table 10. Effect of change in spacing between transverse reinforcement on the ultimate torques and angle of twist of HSC Beams B11 and B12

Specimen	Compressive strength (MPa)	Volume Fraction of Fibers (%)	Spacing (mm)	Ultimate Torque (kN.m)	Percent of Increase (%)	Angle of Twist (ϕ) (rad.)	Percent of Increase (%)
B11	84.8	0.75	100	46.29	---	0.03900	---
B12	84.8	0.75	60	52.03	12.4	0.04200	7.7

These results reveal that the behavior of these beams is similar at the diagonal cracking stage. However, beyond this point, when the diagonal crack crosses the shear reinforcement, the stirrups transmit force from one plane to another. Therefore, the existence of shear reinforcement allows the beam section to redistribute internal forces and restrict the spreading of inclined cracks. The stirrups hold the longitudinal reinforcement in place to increase or maintain the forces carried by the aggregate interlock and the dowel action.

4. Crack Patterns of Tested Beams

The failure mode of the tested beams is depicted in Figure 14. Beam B1 (control beam) exhibits standard torsion failure behavior, with spiral diagonal cracks noted continuously across the beam's cross-section with a crack angle of approximately 45° to the longitudinal beam axis. After the load increases, the concrete is crushed in the center of the beam, causing it to fail. This failure mode is typical of beams without steel fibers. Beams with steel fibers, on the other hand, fail differently, particularly those with a high 0.75 steel fiber fraction. The key advantage of steel fiber is that it can create a crack-control system that prevents pseudo-ductility in post-cracking action. The increase in the beam primary cracking strength is called a secondary effect of steel fiber, and it is proportional to the fraction of steel fiber in the concrete blend. For a low fraction of steel fiber, the improvement of primary cracking was slight. The improvement of the first cracking and Tu depended upon the recycled aggregate, which caused them to be clearly improved.

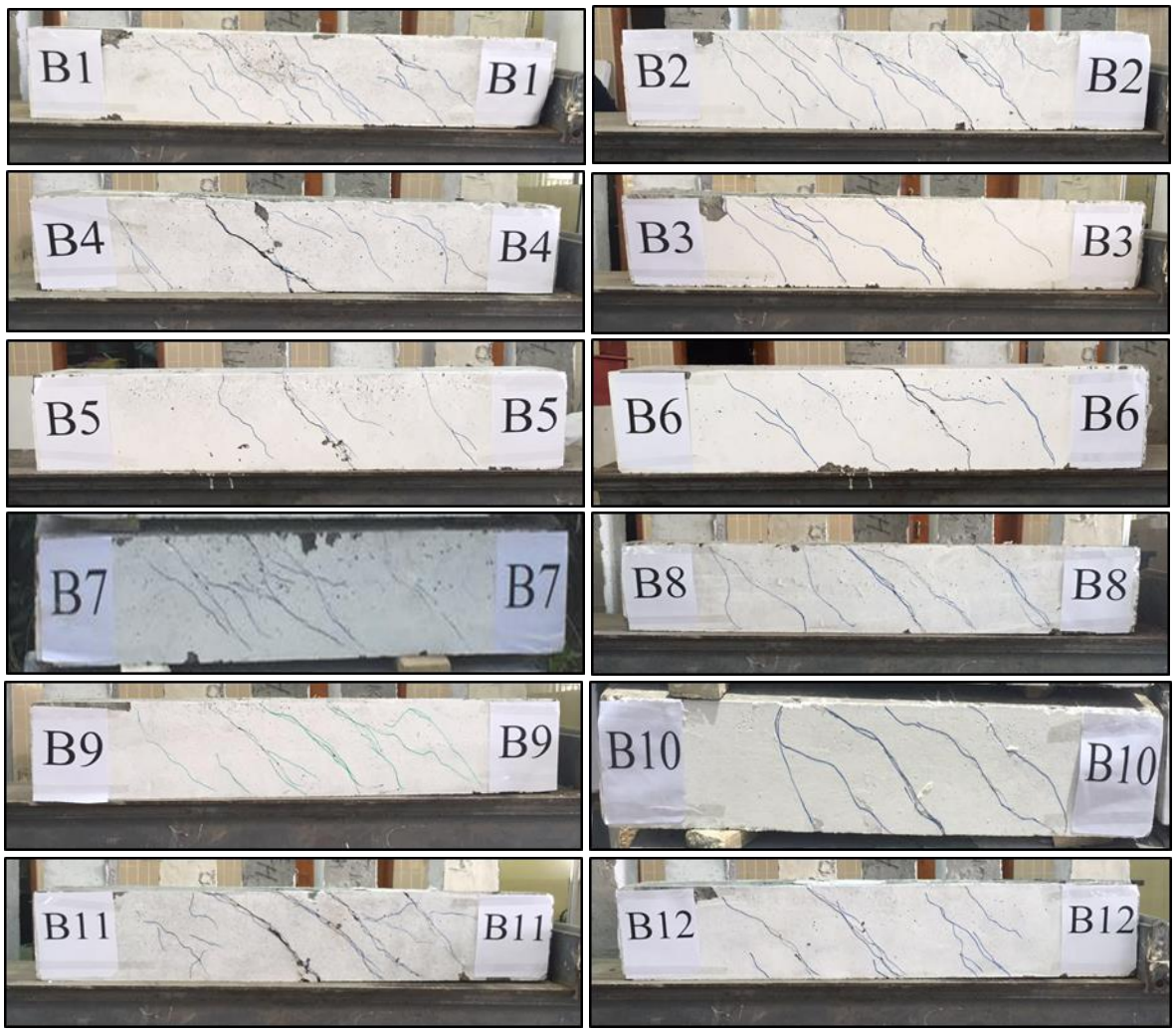

Figure 14. The crack patterns of all tested beams

In the high-strength concrete beams, the cracks pass through the aggregates and are expected to produce a smooth surface. From the test results, it can be observed that the ultimate torsional strength increased as the compressive strength of concrete increased. Also, the rate of this increase in ultimate torsional strength increased as the steel fiber volume fraction increased. It was noticed that when used steel fibers, the crack development became more gradual so that it showed remarkable post-cracking load capacity before failure. In non-steel fibers beams, the formation of an inclined crack was regarded as the dominant feature of the beam's failure mechanism. It was observed that in beams with fibers, larger and more cracks counted for a beam at failure stage, and the crack width was less than for non-fibrous beams. Several cracks were observed in all fibrous beams with a relatively high percentage of steel fibers, indicating the redistribution of stresses beyond cracking. The steel fibers became effective after the formation of the cracks and continued to resist the principal tensile stresses until the complete pull-out of all fibers occurred at one critical crack. Figure 14 shows the crack patterns of all beams.

5. Conclusion

In this study, the effect of steel fibers on the behavior of high-strength reinforced concrete beams under torsion was investigated experimentally. The results found that the effect of the fibers on concrete strength was significant when the concrete strength increased to 84.4 MPa. The ultimate strength increased by 70.2%, and the ultimate torque increased by 110.8% when adding 75% fibers to the concrete mixture when the compressive strength of concrete was 84.8 MPa and spacing between transverse reinforcements was 60 mm. Increasing the compressive strength of the section decreases the twist angle. The results found that adding steel fibers to concrete increased the cracking strength, and the ultimate torsional strength increased by 27.1% when 75% steel fibers were used. However, there was a slight effect on the torsional stiffness and the ductility of the beam. Also, the ultimate torque was affected by the amount of the transverse reinforcement. It was found that decreasing the spacing between the transverse reinforcements increased the ultimate torque by 19.9% when the spacing decreased to 100 mm. In addition, the torsional stresses and deformations of the reinforced concrete beams were enhanced by increasing the shear reinforcement. The presence of steel fibers will decrease the crack propagation, which becomes more gradual. In non-fibrous concrete beams, the formation of an inclined crack was regarded as the dominant beam failure mechanism. Also, the number of cracks at failure was greater, and the crack width was smaller for fibrous beams compared to non-fibrous beams. Fibrous beams resisted the principal tensile stresses until the complete pull-out of all fibers occurred at a critical crack. Several cracks were observed in all fibrous beams having a relatively high percentage of steel fibers, indicating the redistribution of stresses beyond cracking. The steel fibers became effective after crack formation and continued until eventual failure.

6. Declarations

6.1. Author Contributions

Conceptualization, H.K.H. and M.S.Z.; methodology, H.K.H. and M.S.Z.; validation, H.K.H., M.S.Z. and M.A.A.; formal analysis, H.K.H.; investigation, M.S.Z.; resources, H.K.H. and M.A.A.; data curation, M.S.Z. and M.A.A.; writing—original draft preparation, H.K.H.; writing—review and editing, H.K.H.; visualization, M.S.Z. and M.A.A.; supervision, H.K.H. and M.A.A.; project administration, H.K.H.; funding acquisition, H.K.H., M.S.Z. and M.A.A. All authors have read and agreed to the published version of the manuscript.

6.2. Data Availability Statement

The data presented in this study are available in article.

6.3. Funding and Acknowledgements

The authors are grateful to the Civil Engineering Department of the University of Basrah Engineering College (Iraq) for financial support. Additional thanks go to the technical staff of the Laboratory of the Civil Engineering Department, where the tests were conducted.

6.4. Conflicts of Interest

The authors declare no conflict of interest.

7. References

[1] ACI Committee 544. (1988) State-of-the-art on fiber reinforced concrete. ACI manual of concrete practice. American Concrete Institute.

[2] Nanni, A. (1991). Fatigue behaviour of steel fiber reinforced concrete. Cement and Concrete Composites, 13(4), 239–245. doi:10.1016/0958-9465(91)90029-H.

[3] Eik, M., Puttonen, J., & Herrmann, H. (2015). An orthotropic material model for steel fibre reinforced concrete based on the orientation distribution of fibres. Composite Structures, 121, 324–336. doi:10.1016/j.compstruct.2014.11.018.

[4] Islam, M. S., & Alam, S. (2013). Principal Component and Multiple Regression Analysis for Steel Fiber Reinforced Concrete (SFRC) Beams. International Journal of Concrete Structures and Materials, 7(4), 303–317. doi:10.1007/s40069-013-0059-7.

[5] Srikar, G., Anand, G., & Suriya Prakash, S. (2016). A Study on Residual Compression Behavior of Structural Fiber Reinforced Concrete Exposed to Moderate Temperature Using Digital Image Correlation. International Journal of Concrete Structures and Materials, 10(1), 75–85. doi:10.1007/s40069-016-0127-x.

[6] Ju, H., Lee, D. H., Hwang, J. H., Kang, J. W., Kim, K. S., & Oh, Y. H. (2013). Torsional behavior model of steel-fiber-reinforced concrete members modifying fixed-angle softened-truss model. Composites Part B: Engineering, 45(1), 215–231. doi:10.1016/j.compositesb.2012.09.021.

[7] Chalioris, C. E., & Karayannis, C. G. (2009). Effectiveness of the use of steel fibres on the torsional behaviour of flanged concrete beams. Cement and Concrete Composites, 31(5), 331–341. doi:10.1016/j.cemconcomp.2009.02.007.

[8] Song, P. S., & Hwang, S. (2004). Mechanical properties of high-strength steel fiber-reinforced concrete. Construction and Building Materials, 18(9), 669–673. doi:10.1016/j.conbuildmat.2004.04.027.

[9] Hameed, A. A., & Al-Sherrawi, M. H. (2018). Influence of Steel Fiber on the Shear Strength of a Concrete Beam. Civil Engineering Journal, 4(7), 1501. doi:10.28991/cej-0309190.

[10] Denisiewicz, A., Socha, T., Kula, K., & Pasula, M. (2018). Influence of Steel and Polypropylene Fibers Addition on Selected Properties of Fine-Grained Concrete. Civil and Environmental Engineering Reports, 28(4), 138–148. doi:10.2478/ceer-2018-0057.

[11] Zhong, A., Sofi, M., Lumantarna, E., Zhou, Z., & Mendis, P. (2021). Flexural Capacity Prediction Model For Steel Fibre-Reinforced Concrete Beams. International Journal of Concrete Structures and Materials, 15(1). doi:10.1186/s40069-021-00461-0.

[12] Facconi, L., Minelli, F., Ceresa, P., & Plizzari, G. (2021). Steel fibers for replacing minimum reinforcement in beams under torsion. Materials and Structures/Materiaux et Constructions, 54(1). doi:10.1617/s11527-021-01615-y.

[13] Lau, C. K., Htut, T. N. S., Melling, J. J., Chegenizadeh, A., & Ng, T. S. (2020). Torsional behaviour of steel fibre reinforced alkali activated concrete. Materials, 13(15), 1–20. doi:10.3390/ma13153423.

[14] American American Specification for Testing and Materials, (1990) "Making and Curing Concrete Test Specimens in the Laboratory," C192-1990.

[15] American Specification for Testing and Materials, (1993) "Test for Compressive Strength of Cylinder Concrete Specimens," C39-1993.

[16] American Specification for Testing and Materials, (1990) "Test for Splitting Tensile Strength of Cylindrical Concrete Specimens," C496-1990.

[17] Iraqi Specification No. 5, (984) "Portland Cement," Baghdad, Iraq.

[18] Iraqi Specification No. 45. (1984). Natural Sources for Gravel that is Used in Concrete and Construction. In Baghdad, Iraq.

[19] ASTM C33/86 (1986) Standard Specification for Concrete Aggregates, ASTM International.